



Technology assessment of solar disinfection for drinking water treatment

Inhyeong Jeon¹, Eric C. Ryberg¹, Pedro J. J. Alvarez² and Jae-Hong Kim¹✉

Poor access to safe drinking water is a major sustainability issue for a third of the world's population, especially for those living in rural areas. Solar disinfection could be the choice of technology considering the abundant sunlight exposure in infrastructure-limited regions. However, despite recent technological advances, it remains unclear which solar disinfection option is more broadly applicable and reliable, enabling the most efficient use of solar radiation. Here we examine the potential of five most typical solar-based, point-of-use water disinfection technologies, including semiconductor photocatalysis to produce hydroxyl radical, dye photosensitization to produce singlet oxygen, ultraviolet irradiation using light-emitting diodes powered by a photovoltaic panel, distillation using a solar still and solar pasteurization by raising the bulk water temperature to 75 °C. The sensitivity analysis allows us to assess how pathogen type, materials property, geographical variation in solar intensity and water-quality parameters interactively affect the effectiveness of these technologies under different scenarios. Revealed critical challenges point to the large gap between idealized materials properties and state of the art, the risk of focusing on select pathogens that show maximum inactivation effectiveness and the failure to consider uncertainties in water quality and geographical variations. Our analysis also suggests future pathways towards effective solar disinfection technology development and real-world implementation.

Over 600 million people living in rural areas of low- to medium-income countries (LMICs) still lack access to basic drinking water services (an improved drinking water source that can be collected within 30 minutes of travel time)^{1–3}. Waterborne infectious diseases continue to be the most prevalent cause of diarrhoeal morbidity and mortality in these regions^{4,5}. The standard approach to provide safe potable water in urban areas has been centralized water treatment along with water distribution networks. For many sparsely populated rural communities, however, centralized water treatment and distribution is not a viable solution because of the lack of basic infrastructure and the high investment and maintenance cost. Consequently, point-of-use (POU) water treatment technologies have been extensively pursued as an alternative due to their relatively low cost, simple operation and proven effectiveness for reducing diarrhoeal disease burden^{6,7}.

It is noteworthy that regions with limited access to basic drinking water services largely overlap with areas receiving high surface sunlight intensity throughout the entire year⁸. Our analysis suggests that, among countries reporting less than 80% access to basic drinking water services in rural populations, the top 10% sunniest countries (the top 20 of 197 countries with both solar irradiation data and drinking water service access data) receive an average solar irradiation of 6.04 kWh m⁻² d⁻¹ (Supplementary Note 1 and Supplementary Fig. 1). This value is significantly greater than the global average of 4.70 kWh m⁻² d⁻¹ (28% greater, $P < 0.0001$). Further, rural populations of these countries have only 48% access to basic drinking water services, leaving 160 million rural residents of these 20 countries without access to a basic drinking water service. Therefore, solar-based POU water treatment technologies are primed to take advantage of abundant solar resources and expand access to potable water.

Solar disinfection (SODIS), the practice of simply exposing polyethylene terephthalate bottles containing water to sunlight, has been

the benchmark of near-zero-cost POU technologies⁹. However, only a small portion of the solar spectrum (ultraviolet A (UVA)) promotes disinfection by SODIS, and it takes upward of 30 hours of sunlight exposure to achieve 3-log (99.9%) inactivation of some viruses under typical weather conditions¹⁰. To better exploit solar energy, more advanced POU disinfection technologies have been explored^{8,11}, such as photocatalysts or photosensitizers to produce reactive oxygen species (ROS) and germicidal UV light-emitting diodes (LEDs) connected to photovoltaic (PV) cells. Technologies that convert solar irradiation to heat energy for localized heating of a pathogen-contacting surface^{12,13}, pasteurization by bulk water heating^{14–17} and distillation and steam generation have also been developed^{18–20}, and some are starting to be translated into commercial POU technologies^{7,21}. Despite notable advances in the field, there is a dearth of information on how various solar POU technologies compare with each other in terms of best utilizing the solar irradiation and their broad applicability. Even when the energy input (solar irradiation) is fixed, such a comparison is often difficult due to the use of unrealistically strong irradiation in many studies. Different technologies require distinct types of pretreatment to remove interfering water constituents as well as pathogens that are not readily inactivated by the technology of choice. Different studies employ different target pathogens, and their selection is often driven by those already proven effective with the chosen disinfection approach. By contrast, the ineffectiveness of a specific technology for the inactivation of other pathogens is often not clearly acknowledged. These limitations distract current research efforts from focusing on issues that are most relevant to the ultimate goal of practical application.

In this study, we critically compare the performance of solar-based POU technologies as a function of geographic location across the globe under both ideal conditions (theoretical maximum) and more realistic conditions (considering the factors that limit

¹Department of Chemical and Environmental Engineering, Yale University, New Haven, CT, USA. ²Department of Civil and Environmental Engineering, Rice University, Houston, TX, USA. ✉e-mail: jaehong.kim@yale.edu

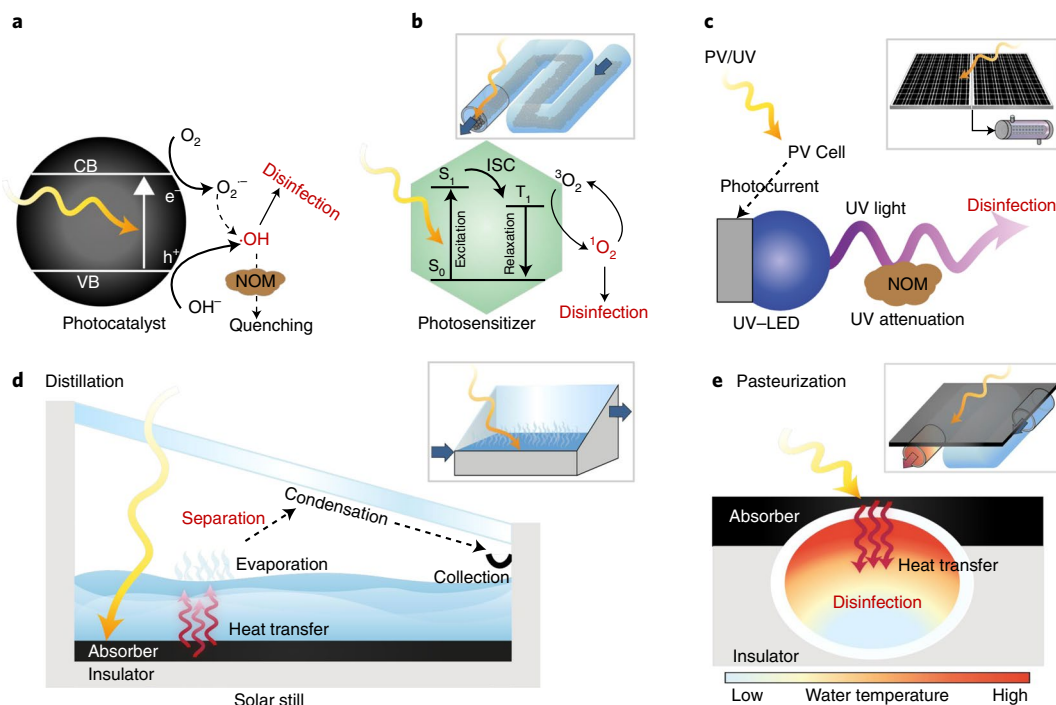


Fig. 1 | Solar-based POU technologies examined in this study. All insets show the overall reactor design and a wavy yellow/orange arrow representing solar radiation. **a**, In photocatalysis, semiconductors with band gaps in the UV and visible range absorb solar photons and produce electron-hole pairs. Through oxidation or reduction pathways, $\bullet\text{OH}$ is formed^{42–44}. **b**, In photosensitization, photosensitizers absorb solar photons with energy within the absorption band and produce $^1\text{O}_2$ by the energy transfer to ground-state $^3\text{O}_2$ (ref. 48). Organic photosensitizers absorb light and become excited to the singlet excited state, then subsequently perform intersystem crossing to create the triplet excited state and finally generate $^1\text{O}_2$ through a Dexter energy transfer. **c**, In PV/UV, PV solar cells are used to absorb sunlight to generate a photocurrent, and the electrons are injected into the LED. The recombination of electrons and holes at a p-n junction generates UV radiation⁷⁴. **d**, In distillation, a solar still is composed mainly of a solar-absorbing plate (basin plate), a glass cover and an insulator. Solar flux is absorbed on the absorber, and heat is transferred to water. Because of the temperature gradient, water vapour is generated through evaporative heat transfer, which is condensed on the surface of the glass cover and finally collected. **e**, In pasteurization, similar to distillation, absorbed solar energy is transferred to water in serpentine tubes, increasing water temperature and thermally inactivating pathogens.

their performance, such as limitations in material properties and water-quality parameters, such as natural organic matter (NOM)). We choose five solar POU water disinfection systems on the basis of their prevalence in research and the disparate mechanisms they employ: photocatalysis, photosensitization, PV/UV, distillation and pasteurization. We focus only on the disinfection efficiency as a metric of performance, recognizing that the most serious health risk for the rural areas of LMICs results from waterborne infectious diseases^{4,5}. We also choose different classes of pathogens and perform a comprehensive sensitivity analysis to discern the unique challenges and opportunities of each technology. Our results highlight the risk of using a single pathogen and idealized conditions to evaluate disinfection capacity of these technologies, and they further clarify the challenges and prospects of solar-based POU disinfection technology development.

Results

Global potential of disinfection capacity. ‘Disinfection capacity’ ($\text{lm}^{-2}\text{day}^{-1}$) is defined in this study as the amount of disinfected water produced by each solar-based POU technology that captures sunlight over a unit area at Earth’s surface. Schematic diagrams of the five solar-based POU technologies are shown in Fig. 1. A detailed procedure to calculate the disinfection capacity for each technology is described in Supplementary Notes 3–8. The calculated disinfection capacities for different POU technologies in both ideal and realistic cases are shown in Fig. 2a,b. These values represent the maximum amount of disinfected water in each case that can be

produced from water that contains a wide range of pathogens, from viruses to protozoa, without pretreatment. In the ideal condition, the disinfection capacity represents the theoretical maximum water production with assumptions that the properties of materials reach their maximum design goals and 100% of solar energy is used to disinfect water without any energy loss. The disinfection capacity in this case is, therefore, the idealized upper boundary of each technology, which is not likely to be reached. It is still useful to compare the ceiling potential of each option since the optimism towards such idealized goals has often motivated extensive research investment in the past. By contrast, disinfection capacity in the realistic case (Fig. 2b) is calculated on the basis of the known properties of existing materials. Consequently, it represents the maximum disinfection capacity that can be achieved with currently available materials and technologies. All underlying assumptions, including material properties, are summarized in Supplementary Table 3.

In ideal cases, all solar-based POU technologies, except distillation, have a relatively high disinfection capacity, more than $80\text{lm}^{-2}\text{d}^{-1}$ in most regions across the globe. Distillation is a clear outlier in this set of simulations; it produces less than $51\text{m}^{-2}\text{d}^{-1}$ even in the ideal situation due to the high energy required for water vaporization^{22,23}. Direct comparison with other disinfection technologies is not warranted since distillation is used primarily for desalination and is the only technology that can be used in regions where a freshwater source is not available. Regardless, this result highlights that POU solar distillation is much less efficient when water production per surface area is considered and

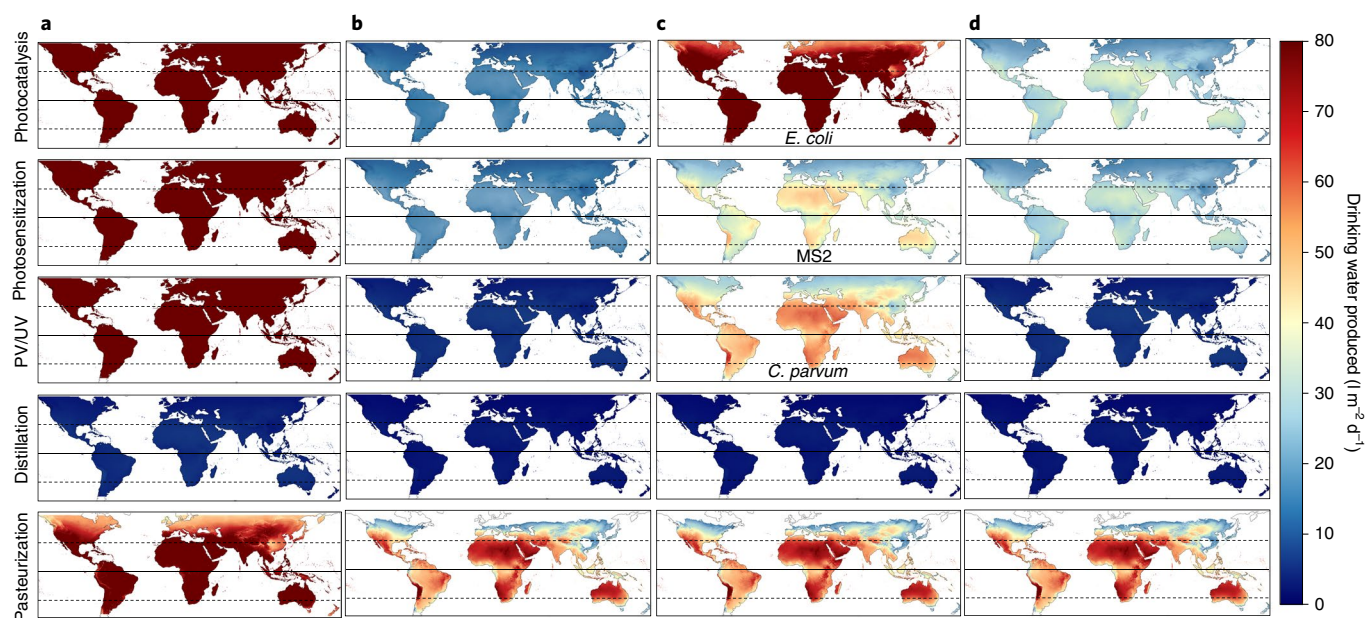


Fig. 2 | Global mapping of disinfection capacity by each solar-based POU technology in various cases. **a, b**, The disinfection capacities of solar non-thermal POU technologies without pretreatment in the ideal (**a**) and realistic (**b**) cases are calculated by considering the most resistant pathogens to disinfection, which are *C. parvum* oocysts, *E. coli* and MS2 for photocatalysis, photosensitization and PV/UV, respectively. **c**, The disinfection capacity in the realistic case with hypothetical pretreatment is calculated under the situation where water contains only the most vulnerable pathogen to each technology, which is *E. coli*, MS2 and *C. parvum* oocysts, for photocatalysis, photosensitization and PV/UV, respectively. **d**, The disinfection capacity in the realistic case with a commercially available ceramic pot filter for pretreatment is calculated with assumptions that 2.3-log removal of bacteria and more than 2-log removal of *C. parvum* oocysts can be achieved by filtration, while virus removal by filtration is not effective. The global mapping of pasteurization in **c** and **d** are underestimated here because we did not consider a decrease in the required contact time resulting from the reduced pathogen load caused by pretreatment, which eventually increases disinfection capacity. The centre line represents the Equator, and the upper and lower dotted lines represent 30° N and 30° S, respectively.

is not likely reasonable to consider if disinfection is the primary treatment target. Therefore, our subsequent comparative analysis excludes solar distillation.

Under realistic scenarios, photocatalysis and photosensitization systems exhibit average disinfection capacities of 15 and 18 l m⁻² d⁻¹, respectively, in the latitude range from 30° S to 30° N where SODIS is recommended²⁴. By contrast, PV/UV shows a relatively small disinfection capacity of 4.5 l m⁻² d⁻¹. We note that there are substantial differences in disinfection capacities between ideal and realistic cases, particularly in these non-thermal POU technologies: photocatalysis, photosensitization and PV/UV. This is mainly because of the large gap between properties of idealized materials and those of available materials (for example, low quantum yield (QY) of photocatalysts²⁵ and low external quantum efficiency of UV-emitting LEDs^{26–28}). Many past studies focusing on materials-based approaches are built on the anticipation that this theoretical maximum can be reached by continued research. Unfortunately, the progress towards this goal has been relatively slow. There still exist many technical challenges, often at the level of a material's property limitations, that make technology implementation in real practice far from reality, despite the optimism accumulated in scientific literature. The slow translation to practice has even been causing such optimism to be criticized as academic hype²⁵. Compared with these technologies, solar pasteurization is much less dependent on the breakthroughs in materials^{19,20} and achieves a much larger disinfection capacity of 58 l m⁻² d⁻¹ on average in the same latitudinal range from 30° S to 30° N.

Results of sensitivity analysis. The global mapping (Fig. 2a,b) represents a conservative scenario in which the disinfection capacities are determined by the most resistant pathogen against each technology (for example, *Cryptosporidium parvum* oocysts for [•]OH,

Escherichia coli for ¹O₂ and MS2 phage for UV). The mapping is also based on fixed values for various input factors, including the CT or IT values (the product of disinfectant dose, concentration (C) of chemical disinfectant or intensity (I) of germicidal UV irradiation, and the exposure time (T)) and the concentration of NOM, an ROS scavenger and UV absorbent. However, in real practice, many parameters affecting the disinfection capacity have large variability and uncertainty. Consequently, the disinfection capacity should be approached statistically and described as a distribution, not as a fixed value. We consider this uncertainty as one of the major concerns for the real-world application of POU technologies. Recently, Morris one-at-a-time screening analysis and Sobol's variance-based sensitivity analysis have been employed to evaluate various factors influencing sunlight inactivation of viruses²⁹. In this study, we apply these two sensitivity analyses to determine how each parameter influences the disinfection capacity and contributes to the overall prediction of uncertainty. All input parameters used in sensitivity analyses are summarized in Supplementary Note 10 and Supplementary Table 10. Focusing our efforts on regions where solar POU technologies are most likely to be applied, we examined the top 10% sunniest countries with less than 80% rural access to basic drinking water services as discussed, using the range of sunlight intensity and ambient temperature in these regions.

The normalized Morris index (μ^*) and the normalized Sobol index (S_{Ti}) are shown in Supplementary Fig. 6. It was observed that the trends of μ^* and S_{Ti} among the technologies are fairly similar, meaning that parameters with a larger contribution to the disinfection capacity (higher μ^*) have a greater impact on its uncertainty (higher S_{Ti}) as well. Considering this correlation, we employed only one index, the S_{Ti} , to uncover which parameters have a higher impact on the uncertainty of the disinfection capacity (Fig. 3a). In addition,

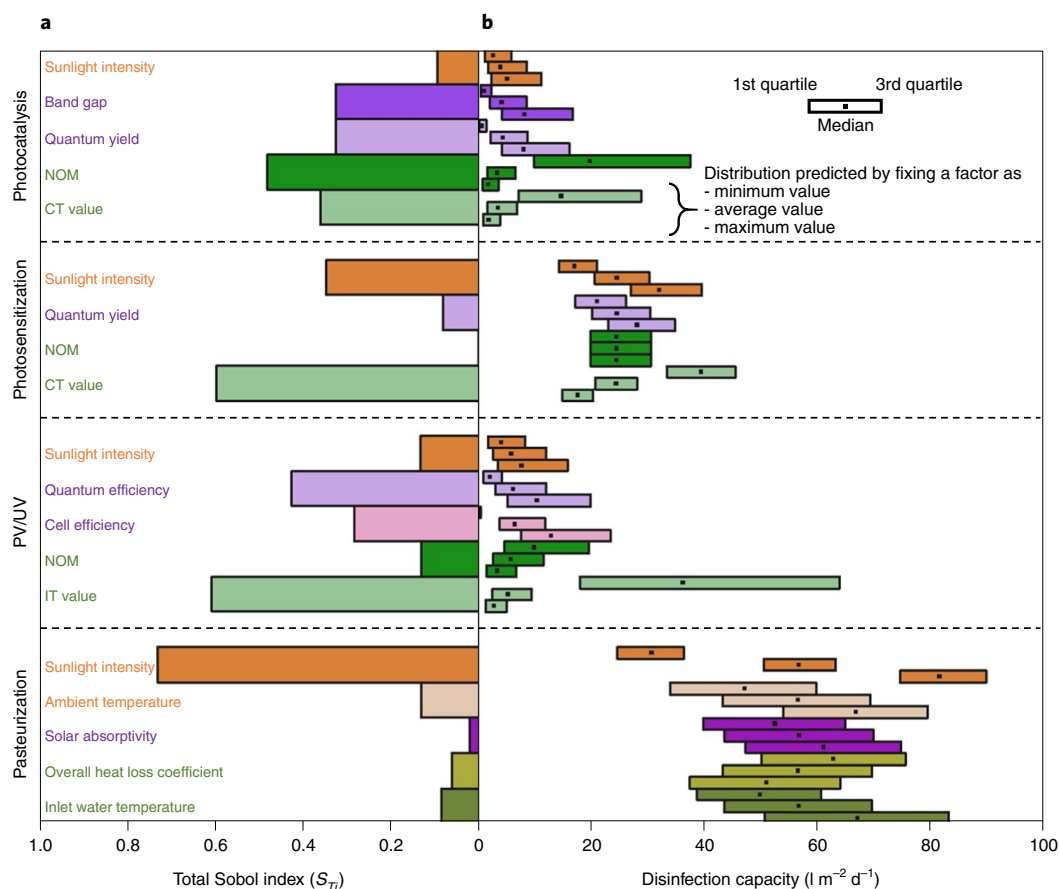


Fig. 3 | Results of sensitivity analyses and Monte Carlo simulations. a, Total Sobol index (S_T) of solar-based POU technologies. All parameters used in the sensitivity analyses are divided into three subgroups: geospatial (orange colour), material (purple colour) and others (green colour). Note that the sensitivity index is a relative value, so it can be used only to compare the uncertainty of parameters within a particular technology. **b**, Box plots of disinfection capacity as a result of Monte Carlo simulations ($n=100,000$). The left and right corners of each box plot represent the first and third quartiles of the predicted distribution, respectively, and the dot in the box represents the median. Three box plots (top, middle and bottom) for every parameter in each POU technology are predicted distributions by Monte Carlo simulations with fixing the parameter as minimum, average and maximum value, respectively, while all other parameters are not fixed.

we examined the distribution of disinfection capacity in three representative cases where only one parameter is set to be the minimum, average and maximum value within the range, while keeping other parameters constant by Monte Carlo simulations (Fig. 3b). In the following, we analyse the simulation results for each POU technology.

(1) **Photocatalysis.** The geospatial factor, or sunlight intensity, has a relatively small effect on the uncertainty of the disinfection capacity, accounting for 6% of the overall uncertainty. By contrast, the material properties such as band gap and QY have a substantial impact on the uncertainty (41% in total), accounting for 20% and 21%, respectively. Other parameters, such as the concentration of NOM and CT values, have a slightly greater influence in the total uncertainty (53% in total), accounting for 30% and 23%, respectively. Consistently, large differences in the three box plots of each of these parameters were observed (Fig. 3b), and the median disinfection capacity under the best condition for a given parameter was about eight times larger than that under the worst condition. The dispersion of the distribution, expressed in terms of the interquartile range (IQR), was also eight times greater; for example, the disinfection capacity ranged from 1 to $41 l m^{-2} d^{-1}$ at the maximum CT value (worst condition), while it ranged from 7 to $291 l m^{-2} d^{-1}$ at the minimum CT value (best condition).

(2) **Photosensitization.** Contrary to the other non-thermal technologies, the geospatial factor has a high impact on the uncertainty of disinfection capacity, accounting for 34%, while the material factor, QY, has a fairly small impact, accounting for only 8% of the uncertainty. Unlike photocatalysis, the uncertainty caused by the concentration of NOM is not outstanding, accounting for 1%, because of the relatively low reactivity of the mild oxidant 1O_2 with NOM³⁰. Interestingly, 58% of the uncertainty is attributed to the CT value, and therefore, the differences in the three box plots obtained by changing CT values in Fig. 3b is the largest of the parameters. This large variation is due to the disparity in the effectiveness of 1O_2 for the inactivation of different pathogens and specific pathogen–photosensitizer interactions⁸. The median disinfection capacity was enhanced more than two times under the best condition compared with the worst condition, from 18 to $40 l m^{-2} d^{-1}$.

(3) **PV/UV.** Sunlight intensity has a negligible effect on the uncertainty in the target countries, around 8%, while material factors, including cell efficiency and external quantum efficiency, greatly affect the uncertainty, 18% and 27%, respectively. Similar to photosensitization, the concentration of NOM and its impact on UV transmission have a relatively small effect on uncertainty, while IT values have the greatest contribution on the uncertainty, around 38%. The median disinfection capacity

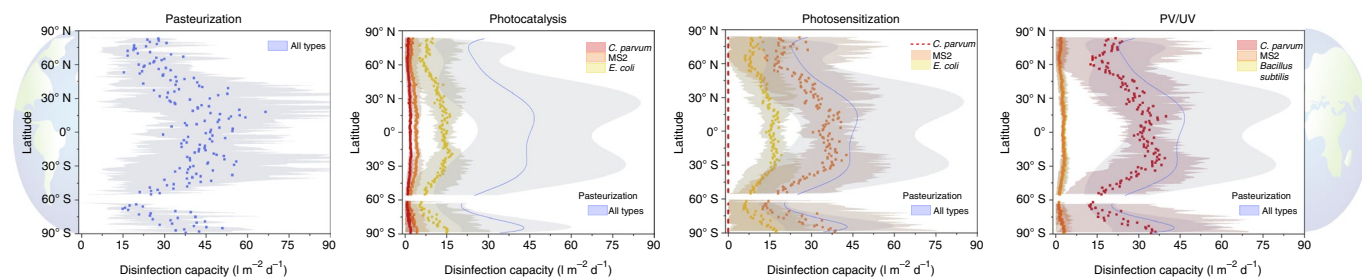


Fig. 4 | Range of disinfection capacity of solar-based POU technologies by various types of pathogens, latitude and month. Dots in each figure represent the median disinfection capacity among 12 months from the Monte Carlo simulations ($n=100,000$) using monthly average sunlight intensity and temperature, while shaded regions mark a range between a minimum monthly median (winter) and a maximum monthly median (summer) value of disinfection capacity that reflects monthly changes in sunlight intensity and temperature (Supplementary Fig. 7). Different colours in the non-thermal technologies (yellow, orange and red) represent the disinfection capacity against different types of pathogens (bacteria, viruses and protozoa). The blue lines in the case of non-thermal technologies show trend lines of the median disinfection capacity of pasteurization (blue dots), while the blue shaded area represents the range between a trend line of the minimum monthly median (winter) and maximum monthly median (summer) value. The break near 60°S represents that there is no continental land area. In photosensitization, although there is no information on CT value against *C. parvum*, the removal efficiency is assumed to be nearly zero due to its high resistance to exogenous inactivation by photosensitization^{47,75}, which is shown as a red dotted line. In PV/UV, IT values of the most resistant bacteria and viruses in Supplementary Table 3 are used to predict disinfection capacity.

greatly increased—more than 12 times—under the best condition compared with the worst condition, and the dispersion of the distribution increased as well. For example, the disinfection capacity ranged from 1 to $51\text{ m}^{-2}\text{ d}^{-1}$ with the maximum IT value, while it ranged from 18 to $641\text{ m}^{-2}\text{ d}^{-1}$ with the minimum IT value.

- (4) **Pasteurization.** The geospatial factors, sunlight intensity and ambient temperature, have a substantially large effect on the uncertainty (83% in total) for pasteurization compared with other technologies. In particular, variation in sunlight intensity depending on the time of the year and meteorological conditions (Supplementary Note 10) plays an important role in its uncertainty, accounting for 71%. Nevertheless, the median disinfection capacity under the worst temporal condition for sunlight intensity (winter) was $311\text{ m}^{-2}\text{ d}^{-1}$, which is still high for household-scale water treatment. The median disinfection capacity under the best condition (summer) is as high as $821\text{ m}^{-2}\text{ d}^{-1}$, which is the largest among all conditions for all the POU technologies analysed.

Although it appears as if pasteurization exhibits the largest uncertainty among the technologies due to sunlight intensity variation because of its high IQR, note that the IQR should not be used as the sole measure to compare the degree of uncertainty among different distributions. The variability of a distribution depends highly on the magnitude of the centre of each distribution, and therefore, instead of the IQR, the ratio of the IQR to the median (IQR/M) is a more representative measure of the uncertainty of a distribution. We find that pasteurization has the smallest IQR/M for sunlight intensity around 0.26, while the IQR/M ratios of photocatalysis, photosensitization and PV/UV are 1.66, 0.40 and 1.55, respectively. This indicates that although sunlight intensity had the greatest impact on the absolute uncertainty for pasteurization, its relative uncertainty considering the scale of disinfection capacity was the smallest among all of the technologies. Material factors such as solar absorptivity have a small impact on the uncertainty, around 2%. Other factors, including the overall heat loss and inlet water temperature, account for 6% and 8% of uncertainty, respectively. For all factors except sunlight intensity, the minimum disinfection capacity for pasteurization under the worst conditions is $341\text{ m}^{-2}\text{ d}^{-1}$, which is still higher than that of the other POU technologies under their best conditions.

The preceding results suggest that the types of pathogens, and accordingly their CT or IT values, would be the most important parameter in determining the uncertainty in all non-thermal

POU technologies. Note that many relevant studies focus only on pathogens that show the maximum inactivation effectiveness when testing disinfection performance. For example, if we assume that photocatalysis, photosensitization and PV/UV technologies are used to disinfect water containing only *E. coli*, MS2 and *C. parvum* oocysts, respectively, which are the most susceptible microorganisms or surrogate virus against each technology, their disinfection capacities would be remarkably increased as shown in Fig. 2c. Such narrow focus is not completely impossible, if pretreatment provides an absolute barrier for other pathogens that are not well treated in the disinfection step. In reality, there is often a lack of pretreatment (for example, ceramic pot filtration and sand filtration). Even if pretreatment is present, it does not provide a reliable barrier, which is often the case in remote applications in the absence of proper maintenance and local expertise³¹. Consequently, the technologies developed using particular pathogens as their target could overestimate their disinfection capacity or become excessively dependent on the performance of pre- or post-treatment. The same concern is reflected in World Health Organization guidelines in which the disinfection performance of a POU technology is evaluated on the basis of the simultaneous removal of all three types of pathogens (bacteria, viruses and protozoa)^{7,21}.

It is also noteworthy that materials play an important role in determining the overall performance and uncertainty for materials-based approaches, including photocatalysis and PV/UV. Water-quality variations, as exemplified by NOM, are also one of the contributors to the performance and uncertainty for these technologies. Note that we have not included the impact of turbidity variation, and therefore, the actual disinfection capacity of photocatalysis and PV/UV without pretreatment could be smaller than predicted values. Among the POU technologies examined, pasteurization shows the smallest uncertainty depending on the types of pathogens, materials and water constituents, with the highest median value of disinfection capacity in the average case, which indicates the potential of pasteurization as the most promising technology to provide biologically safe drinking water in LMICs.

Latitudinal and monthly variations. Considering the large dependency of disinfection capacity on the types of pathogens present (for non-thermal technologies) and geospatial factors (for pasteurization), we expanded the Monte Carlo simulation as a function of latitudinal location across the globe as a function of both the types of pathogens and the time of year (Supplementary Note 12 and Supplementary Table 12). Considering that the distribution of

disinfection capacity varies more with latitude than with longitude, we performed the Monte Carlo simulations ($n = 100,000$) as a function of month by using the monthly average sunlight intensity and temperature data at each specific latitude (Supplementary Note 13 and Supplementary Fig. 7). Minimum and maximum monthly median values among all 12 months correspond to the shaded regions in Fig. 4, while each dot represents the median disinfection capacity for every latitude among all 12 months. Here we used the disinfection capacity of pasteurization as a baseline for comparison, where the blue shaded areas and lines in plots of non-thermal technologies in Fig. 4 depict the minimum, median and maximum monthly disinfection capacity of pasteurization by each latitude. In the latitudinal range between 30°S and 30°N , the first-quartile value of disinfection capacity during the winter was $171\text{m}^{-2}\text{d}^{-1}$ for pasteurization; this was slightly smaller than what we expected in Fig. 3, which was around $241\text{m}^{-2}\text{d}^{-1}$, because of the wider range of sunlight intensity and temperature used for this analysis. However, the winter median disinfection capacity in those regions was still reasonably high, around $221\text{m}^{-2}\text{d}^{-1}$, which highlights that most countries between 30°S and 30°N would be capable of producing adequate amounts of drinking water even during the winter. In summer, a minimum of $50\text{m}^{-2}\text{d}^{-1}$ of drinking water can be produced, with a median value of $741\text{m}^{-2}\text{d}^{-1}$. The overall result demonstrates that pasteurization has the potential to produce reasonable amounts of water in most regions between 30°S and 30°N regardless of the time of year.

Non-thermal POU technologies had similar latitudinal trends as pasteurization, showing the maximum disinfection capacity near 17°N or 20°S , where the annual temperature and sunlight intensity are the highest (Supplementary Fig. 8), while the monthly variation is less substantial than for pasteurization, which corroborates the results of our sensitivity analyses. However, unlike pasteurization, there were large variations in the disinfection capacity by the type of pathogen. Each technology shows better disinfection efficiency against pathogens with smaller *CT* or *IT* values; that is, *E. coli* for photocatalysis, MS2 for photosensitization, and *C. parvum* oocysts for PV/UV. However, it is difficult to remove only one specific pathogen effectively without removing other pathogens. We modelled the disinfection capacity assuming a scenario where ceramic pot filtration is employed to achieve 2.3-log removal of bacteria and *C. parvum* oocysts (Supplementary Note 14), and the predicted disinfection capacity (Fig. 2d and Supplementary Fig. 9) emphasizes the importance of pretreatment and multi-barrier approaches for solar non-thermal POU disinfection technologies^{7,21}. The results also foreshadow the risks involved in these technologies due to their reliance on successful pretreatment.

Discussion

Our study reveals both the potential and limitations of solar POU disinfection technologies that have been extensively explored over the past decades. We summarized the challenges faced by each solar-based POU technology and what research should be conducted for each technology (Supplementary Note 14). Nevertheless, our study suggests that narrowly focusing on overcoming the unique challenges faced by individual technologies (Supplementary Note 14) cannot meet the goal of simultaneously removing a wide range of pathogens. Many past studies aimed at enhancing disinfection effectiveness against a single specific pathogen as an evaluation measure and achieving marginal improvement in the properties of often futuristic materials based on the optimism of drastic reduction in future cost. This often obscures critical challenges related to the large uncertainties and fair cross-comparison of different technical approaches. Large variations, often more than an order of magnitude (Supplementary Table 1), in the disinfectant dose and the exposure time required depending on the types of pathogens need to be carefully considered in the context of multi-barrier strategies and the availability of proper pretreatment methods. The lack

of *CT* and *IT* values for many pathogens is another notable barrier and the source of uncertainty, and more research is required (Supplementary Note 16). Pasteurization is less affected by such uncertainties in design and environmental factors (Supplementary Notes 13 and 15), but it has received much less attention in research. In all POU technologies, strategies to avoid recontamination of treated water during storage also need to be considered^{3,7,21,32}.

Our focus on technologies does not discount the importance of other challenges that limit their practical implementation, such as economic barriers—in particular, rural–urban inequality. For example, our further analysis suggests that access to basic drinking water services depends on gross domestic product per capita in rural areas more than in urban areas (Supplementary Note 19 and Supplementary Fig. 12). Although LMICs spend a proportional amount of their gross domestic product on improving drinking water, their financial resources—with financial assistance from international organizations considered—remain relatively small on an absolute scale (Supplementary Fig. 13). The rural–urban inequality is further exacerbated by a larger deficiency in funding for rural areas (78%) than for urban areas (39%) for drinking water access, requiring households to contribute 66% of the finances for water, sanitation and hygiene development³³, as well as unequal geographical distribution of wealth, with 80% of the global extreme poor population (individuals earning less than \$1.90 per day) living in rural areas³⁴. It is important to note that, even at the same level of economic prosperity, rural regions have less access to safe drinking water than do urban regions. Even in the case of higher urban poverty rates, urban regions appear somewhat resilient and preserve their access to safe drinking water (Supplementary Note 19 and Supplementary Fig. 14). It is expected that if the current pace of improving water access is kept constant until 2030, it is insufficient to achieve universal access to even basic drinking water services in rural areas, and just one-fourth of countries are on track to achieve >99% access to basic water services⁴. Other societal and cultural barriers limiting user adoption and sustained practice are also profound and need to be resolved^{3,7,21,32,35}. At the same time, to address water problems in rural regions within a reasonable time frame, the low-cost POU technologies discussed in this study are probably a more viable approach than relying on drastic improvements of gross economic status.

Methods

Statistical analysis. Statistical analyses include a comparison of the global insolation with the sunlight intensity of the top 10% sunniest countries with less than 80% rural access to basic drinking water (Supplementary Note 1), investigating which water, sanitation and hygiene service intervention is the most impactful for reducing diarrhoeal mortality (Supplementary Note 18) and the role of economic prosperity in expanding the access to basic drinking water and rural–urban inequality (Supplementary Notes 19 and 20). General details of each statistical analysis and statistics are summarized in Supplementary Note 17 and Supplementary Tables 13 and 14.

Calculation of disinfection capacity. We consider diverse pathogens, including bacteria, viruses and protozoa, responsible for causing waterborne disease^{36–38}. On the basis of US Environmental Protection Agency and World Health Organization regulations and guidelines^{37,39,40}, we set 4-log removal for bacteria and viruses and 2-log removal of protozoan parasites as the minimum requirement for the technology to claim that the water has been disinfected. Notably, different technologies demonstrate different inactivation efficiencies across the types of pathogens^{8,41}. Therefore, we base our calculation on the worst-case scenario where the source water contains all classes of pathogens and proper pre- and post-treatments are not available.

In photocatalysis, semiconductors absorb photons with energy higher than their band gap to produce electron–hole pairs ($e^{-}h^{+}$), which subsequently catalyse the production of ROS such as $\cdot\text{OH}$ (refs. 42–44), the main disinfecting agent in photocatalytic water disinfection (Fig. 1a)^{45,46}. Similarly, in photosensitization, organic photosensitizers catalyse the production of ROS, predominantly $^1\text{O}_2$, upon light absorption (Fig. 1a)^{47,48}. In PV/UV, a PV cell generates a photocurrent and powers a germicidal UV-emitting LED to disinfect water (Fig. 1b). Disinfection capacities of these solar technologies are estimated on the basis of *CT* or *IT* values of each microorganism and virus reported in the literature (Supplementary Table 1). These represent the product of disinfectant dose—concentration (*C*)

of chemical disinfectant or intensity (I) of germicidal UV irradiation—and the exposure time (T). In the case of solar photothermal distillation (water evaporation by solar energy and subsequent vapour condensation), the primary purpose is to desalinate brackish water and seawater. The process also removes most non-volatile constituents as well as all types of microorganisms and viruses. We consider solar distillation as a technology that produces disinfected potable water in regions where saline water is the only available source. The other solar thermal technology, pasteurization, is the process of using solar energy to raise the bulk water temperature above the pasteurization temperature^{17,49,50}. Heat causes damage to biomolecular structures and vital metabolic functions by inducing denaturation and the breakdown of proteins and genomes^{14–17}. Disinfection by heat also varies widely depending on the types of microorganisms/viruses present, as well as temperature and exposure time (Supplementary Table 2)^{51–63}. On the basis of the experimental data in literature, we here assume that raising water temperature above 75 °C for 1 minute achieves 4-log inactivation of all pathogens (Supplementary Fig. 2). A description on the thermal inactivation kinetics and the required temperature and times of pasteurization are summarized in Supplementary Note 2 and Supplementary Table 2. All underlying assumptions used in calculating the disinfection capacity of each technology are summarized in Supplementary Table 3. Details of the specific approaches to calculate disinfection capacities of the five select technologies, along with fundamental modes of their disinfection function, are described in Supplementary Notes 3–8, and parameters used in calculations are summarized in Supplementary Tables 5–9.

Global mapping of disinfection capacity. The yearly average surface solar radiation data (global horizontal irradiance, kWh m⁻² d⁻¹) at a resolution of 30 arcsec between 60° N and 45° S were obtained from the Global Solar Atlas 2.0, a free web-based application developed and operated by Solargis on behalf of the World Bank Group, with funding provided by the Energy Sector Management Assistance Program⁶⁴. We calculate regional disinfection capacities by inputting these regional solar radiation data to the preceding models and plot them on a global map using R⁶⁵.

Sensitivity analysis. We perform Morris one-at-a-time screening analysis and Sobol's variance-based sensitivity analysis to quantitatively evaluate which parameters of the model for each technology have the greatest influence on the overall disinfection capacity and its uncertainty (Supplementary Note 9). The Morris method produces two sensitivity indices, μ^* and σ . Index μ^* represents the overall influence on the disinfection capacity across the range of variations (a parameter with higher μ^* has a greater influence on the disinfection capacity). Index σ indicates the degree of interaction with other factors in influencing the disinfection capacity (a parameter with a higher σ has a greater interaction with other parameters)^{66,67}. Sobol's method produces three sensitivity indices (Supplementary Note 9), and we focused mainly on two of these sensitivity indices, which are the main effect, S_i , and the total effect, S_{Ti} . Index S_i means the proportion of uncertainty that is decreased by fixing a parameter X_i , while index S_{Ti} represents the output uncertainty when only the parameter X_i is not fixed^{68,69}. Thus, index S_{Ti} indicates the proportion of the output uncertainty caused by variability of the parameter X_i and the variability associated with the interaction between the parameter X_i and other parameters. In this study, S_{Ti} is used to evaluate the contribution of the variance of each parameter, rather than S_i , because even parameters with low S_i may have a great contribution of uncertainty caused by the interaction with the other parameters. All sensitivity analyses and Monte Carlo simulations were conducted using R, and the sensitivity indices obtained from the analyses are summarized in Supplementary Table 11.

We performed Monte Carlo simulations ($n = 100,000$) for three different cases where only one parameter is set to be the minimum, average and maximum value within the range, while keeping other parameters fixed. For the parameters that positively contribute to the overall disinfection capacity, each value represents the worst, average or best condition, respectively. By performing Monte Carlo simulations for three different cases, we obtained three box plots (top, middle and bottom plots) shown in Fig. 3b for each parameter. Here the interquartile range, the width of the box plot, represents the degree of dispersion of the distribution for a specific condition. The relative positions of the three boxes for each parameter indicate how the change in this parameter (from minimum to maximum) changes the overall disinfection capacity. Not surprisingly, a parameter with higher normalized sensitivity index (Fig. 3a) tends to have a greater influence and larger uncertainty on disinfection capacity (Fig. 3b).

Reporting summary. Further information on research design is available in the Nature Research Reporting Summary linked to this article.

Data availability

Datasets used in this study were accessed from publicly available sources. Long-term annual average surface solar radiation data (global horizontal irradiance (GHI), kWh m⁻² d⁻¹) from 45° S to 60° N at 30 arcsec resolution was sourced from the Global Solar Atlas 2.0⁶⁴. For the sensitivity analyses and Monte Carlo simulations, the monthly sunlight intensity was obtained from the NASA Langley Research Center Atmospheric Science Data Center Surface Meteorological and Solar Energy (SSE)^{70–72}, which provides the surface sunlight intensity across the globe at

1° latitude by 1° longitude resolution, while the monthly surface temperature was obtained from the Berkeley Earth website (<http://berkeleyearth.org/>). Data pertaining to national, rural and urban access to WASH services, and the rate of change in access, were sourced from the World Health Organization–United Nations Children's Fund (WHO–UNICEF) Joint Monitoring Program⁷, and data reporting the burden of disease/specific diarrhoeal mortality rates for insufficient WASH improvements access was acquired from the WHO Global Health Observatory data repository⁴. Country economic parameters, including poverty metrics, GDP per capita and other measures of wealth were sourced from the World Bank World Development Indicators⁷³, while information on country-specific WASH financing structures and investments were acquired through the United Nations Water Global Analysis and Assessment of Sanitation and Drinking Water^{7,33}.

Code availability

The R software, GraphPad Prism X9 software and the freely available R packages were used for all data exploration and statistical analyses. The codes that support the findings of this study are available from the corresponding author upon reasonable request.

Received: 25 October 2021; Accepted: 17 May 2022;

Published online: 30 June 2022

References

1. Sustainable Development Goal 6: Synthesis Report 2018 on Water and Sanitation (United Nations, 2018).
2. The Millennium Development Goals Report 2015 (United Nations, 2015).
3. Progress on Household Drinking Water, Sanitation and Hygiene 2000–2017: Special Focus on Inequalities (UNICEF and WHO, 2019).
4. Global Health Observatory Data Repository (WHO, accessed 9 June 2022); <https://www.who.int>
5. Montgomery, M. A. & Elimelech, M. Water and sanitation in developing countries: including health in the equation. *Environ. Sci. Technol.* **41**, 17–24 (2007).
6. Combating Waterborne Disease at the Household Level (WHO, 2007).
7. Results of Round II of the WHO International Scheme to Evaluate Household Water Treatment Technologies (WHO, 2019).
8. Chu, C., Ryberg, E. C., Loeb, S. K., Suh, M.-J. & Kim, J.-H. Water disinfection in rural areas demands unconventional solar technologies. *Acc. Chem. Res.* **52**, 1187–1195 (2019).
9. McGuigan, K. G. et al. Solar water disinfection (SODIS): a review from bench-top to roof-top. *J. Hazard. Mater.* **235**, 29–46 (2012).
10. Fisher, M. B., Keenan, C. R., Nelson, K. L. & Voelker, B. M. Speeding up solar disinfection (SODIS): effects of hydrogen peroxide, temperature, pH, and copper plus ascorbate on the photoinactivation of *E. coli*. *J. Water Health* **6**, 35–51 (2008).
11. Shannon, M. A. et al. In *Nanoscience and Technology: A Collection of Reviews from Nature Journals* (ed. Rodgers, P.) 337–346 (World Scientific, 2010).
12. Loeb, S., Li, C. & Kim, J.-H. Solar photothermal disinfection using broadband-light absorbing gold nanoparticles and carbon black. *Environ. Sci. Technol.* **52**, 205–213 (2018).
13. Loeb, S. K. et al. Nanoparticle enhanced interfacial solar photothermal water disinfection demonstrated in 3-D printed flow-through reactors. *Environ. Sci. Technol.* **53**, 7621–7631 (2019).
14. Wigginton, K. R. & Kohn, T. Virus disinfection mechanisms: the role of virus composition, structure, and function. *Curr. Opin. Virol.* **2**, 84–89 (2012).
15. Fraise, A. P., Lambert, P. A. & Maillard, J.-Y. *Russell, Hugo & Ayliffe's Principles and Practice of Disinfection, Preservation and Sterilization* (Wiley & Sons, 2008).
16. McDonnell, G. E. *Antisepsis, Disinfection, and Sterilization: Types, Action, and Resistance* (Wiley & Sons, 2020).
17. Burch, J. D. & Thomas, K. E. Water disinfection for developing countries and potential for solar thermal pasteurization. *Sol. Energy* **64**, 87–97 (1998).
18. Sampathkumar, K., Arjunan, T., Pitchandi, P. & Senthilkumar, P. Active solar distillation—a detailed review. *Renew. Sustain. Energy Rev.* **14**, 1503–1526 (2010).
19. Wang, Z. et al. Pathways and challenges for efficient solar-thermal desalination. *Sci. Adv.* **5.7**, aax0763 (2019).
20. Pang, Y. et al. Solar-thermal water evaporation: a review. *ACS Energy Lett.* **5**, 437–456 (2020).
21. Results of Round I of the WHO International Scheme to Evaluate Household Water Treatment Technologies (WHO, 2016).
22. Velmurugan, V., Gopalakrishnan, M., Raghu, R. & Srihar, K. Single basin solar still with fin for enhancing productivity. *Energy Convers. Manage.* **49**, 2602–2608 (2008).
23. Badran, O. O. & Abu-Khader, M. M. Evaluating thermal performance of a single slope solar still. *Heat Mass Transf.* **43**, 985–995 (2007).
24. Luzzi, S., Tobler, M., Suter, F. & Meierhofer, R. *SODIS Manual: Guidance on Solar Water Disinfection* (Eawag, 2016).

25. Loeb, S. K. et al. The technology horizon for photocatalytic water treatment: sunrise or sunset? *Environ. Sci. Technol.* **53**, 2937–2947 (2019).
26. Hirayama, H., Tsukada, Y., Maeda, T. & Kamata, N. Marked enhancement in the efficiency of deep-ultraviolet AlGaIn light-emitting diodes by using a multi-quantum-barrier electron blocking layer. *Appl. Phys. Express* **3**, 031002 (2010).
27. Shur, M. S. & Gaska, R. Deep-ultraviolet light-emitting diodes. *IEEE Trans. Electron Devices* **57**, 12–25 (2009).
28. Khan, A., Balakrishnan, K. & Katona, T. Ultraviolet light-emitting diodes based on group three nitrides. *Nat. Photonics* **2**, 77–84 (2008).
29. Zhang, X. et al. Global sensitivity analysis of environmental, water quality, photoreactivity, and engineering design parameters in sunlight inactivation of viruses. *Environ. Sci. Technol.* **54**, 8401–8410 (2020).
30. Haag, W. R. & Yao, C. D. Rate constants for reaction of hydroxyl radicals with several drinking water contaminants. *Environ. Sci. Technol.* **26**, 1005–1013 (1992).
31. Brown, J. & Clasen, T. High adherence is necessary to realize health gains from water quality interventions. *PLoS ONE* **7**, e36735 (2012).
32. Trimmer, J. T. et al. Re-envisioning sanitation as a human-derived resource system. *Environ. Sci. Technol.* **54**, 10446–10459 (2020).
33. UN-Water Global Analysis and Assessment of Sanitation and Drinking-Water (GLAAS) 2019 Report: National Systems to Support Drinking-Water, Sanitation and Hygiene: Global Status Report 2019 (WHO, 2019).
34. The United Nations World Water Development Report 2019: Leaving No One Behind (United Nations Educational, Scientific and Cultural Organization, 2019).
35. Enger, K. S., Nelson, K. L., Rose, J. B. & Eisenberg, J. N. The joint effects of efficacy and compliance: a study of household water treatment effectiveness against childhood diarrhea. *Water Res.* **47**, 1181–1190 (2013).
36. Hijnen, W., Beerendonk, E. & Medema, G. J. Inactivation credit of UV radiation for viruses, bacteria and protozoan (oo)cysts in water: a review. *Water Res.* **40**, 3–22 (2006).
37. *Evaluating Household Water Treatment Options: Health-Based Targets and Microbiological Performance Specifications* (WHO, 2011).
38. Kohn, T. & Nelson, K. L. Sunlight-mediated inactivation of MS2 coliphage via exogenous singlet oxygen produced by sensitizers in natural waters. *Environ. Sci. Technol.* **41**, 192–197 (2007).
39. *Guidelines for Drinking-Water Quality* 4th edn (WHO, 2011).
40. *National Primary Drinking Water Regulations: Long Term 2 Enhanced Surface Water Treatment Rule; Final Rule* (US EPA, 2006).
41. Loeb, S., Hofmann, R. & Kim, J.-H. Beyond the pipeline: assessing the efficiency limits of advanced technologies for solar water disinfection. *Environ. Sci. Technol. Lett.* **3**, 73–80 (2016).
42. Liu, B., Zhao, X., Terashima, C., Fujishima, A. & Nakata, K. Thermodynamic and kinetic analysis of heterogeneous photocatalysis for semiconductor systems. *Phys. Chem. Chem. Phys.* **16**, 8751–8760 (2014).
43. Malato, S., Fernández-Ibáñez, P., Maldonado, M. I., Blanco, J. & Gernjak, W. Decontamination and disinfection of water by solar photocatalysis: recent overview and trends. *Catal. Today* **147**, 1–59 (2009).
44. Cho, M., Chung, H., Choi, W. & Yoon, J. Linear correlation between inactivation of *E. coli* and OH radical concentration in TiO₂ photocatalytic disinfection. *Water Res.* **38**, 1069–1077 (2004).
45. Cho, M., Cates, E. L. & Kim, J.-H. Inactivation and surface interactions of MS-2 bacteriophage in a TiO₂ photoelectrocatalytic reactor. *Water Res.* **45**, 2104–2110 (2011).
46. Park, G. W. et al. Fluorinated TiO₂ as an ambient light-activated virucidal surface coating material for the control of human norovirus. *J. Photochem. Photobiol. B* **140**, 315–320 (2014).
47. Nelson, K. L. et al. Sunlight-mediated inactivation of health-relevant microorganisms in water: a review of mechanisms and modeling approaches. *Environ. Sci. Process. Impacts* **20**, 1089–1122 (2018).
48. DeRosa, M. C. & Crutchley, R. J. Photosensitized singlet oxygen and its applications. *Coord. Chem. Rev.* **233–234**, 351–371 (2002).
49. Dobrowsky, P. et al. Efficiency of microfiltration systems for the removal of bacterial and viral contaminants from surface and rainwater. *Water Air Soil Pollut.* **226**, 33 (2015).
50. Dobrowsky, P., Carstens, M., De Villiers, J., Cloete, T. & Khan, W. Efficiency of a closed-coupled solar pasteurization system in treating roof harvested rainwater. *Sci. Total Environ.* **536**, 206–214 (2015).
51. Abraham, J., Plourde, B. & Minkowycz, W. Continuous flow solar thermal pasteurization of drinking water: methods, devices, microbiology, and analysis. *Renew. Energy* **81**, 795–803 (2015).
52. Spinks, A. T., Dunstan, R., Harrison, T., Coombes, P. & Kuczera, G. Thermal inactivation of water-borne pathogenic and indicator bacteria at sub-boiling temperatures. *Water Res.* **40**, 1326–1332 (2006).
53. Sancio, P. et al. *Pasteurisation for Production of Class A Recycled Water: A Report of a Study Funded by the Australian Water Recycling Centre of Excellence* Report No. 1922202665 (Australian Water Recycling Centre of Excellence, 2015).
54. Parry, J. & Mortimer, P. The heat sensitivity of hepatitis A virus determined by a simple tissue culture method. *J. Med. Virol.* **14**, 277–283 (1984).
55. Hewitt, J., Rivera-Aban, M. & Greening, G. Evaluation of murine norovirus as a surrogate for human norovirus and hepatitis A virus in heat inactivation studies. *J. Appl. Microbiol.* **107**, 65–71 (2009).
56. Maheshwari, G., Jannat, R., McCormick, L. & Hsu, D. Thermal inactivation of adenovirus type 5. *J. Virol. Methods* **118**, 141–146 (2004).
57. Strazynski, M., Krämer, J. & Becker, B. Thermal inactivation of poliovirus type 1 in water, milk and yoghurt. *Int. J. Food Microbiol.* **74**, 73–78 (2002).
58. Fujino, T. et al. The effect of heating against *Cryptosporidium* oocysts. *J. Vet. Med. Sci.* **64**, 199–200 (2002).
59. Fayer, R. Effect of high temperature on infectivity of *Cryptosporidium parvum* oocysts in water. *Appl. Environ. Microbiol.* **60**, 2732–2735 (1994).
60. Harp, J. A., Fayer, R., Pesch, B. A. & Jackson, G. J. Effect of pasteurization on infectivity of *Cryptosporidium parvum* oocysts in water and milk. *Appl. Environ. Microbiol.* **62**, 2866–2868 (1996).
61. Jarroll, E. L., Hoff, J. C. & Meyer, E. A. in *Giardia and Giardiasis* (eds Erlandsen, S. L. & Meyer, E. A.) 311–328 (Springer, 1984).
62. Ongerth, J. E., Johnson, R. L., MacDonald, S. C., Frost, F. & Stibbs, H. H. Back-country water treatment to prevent giardiasis. *Am. J. Public Health* **79**, 1633–1637 (1989).
63. Schaefer, F. W., Rice, E. W. & Hoff, J. C. Factors promoting in vitro excystation of *Giardia muris* cysts. *Trans. R. Soc. Trop. Med. Hyg.* **78**, 795–800 (1984).
64. *Global Solar Atlas 2.0* (World Bank Group, 2020); <https://globalsolaratlas.info/>
65. R Core Team. R: A language and environment for statistical computing (R Foundation for Statistical Computing, 2021).
66. Campolongo, F., Cariboni, J. & Saltelli, A. An effective screening design for sensitivity analysis of large models. *Environ. Model. Softw.* **22**, 1509–1518 (2007).
67. Saltelli, A. Sensitivity analysis for importance assessment. *Risk Anal.* **22**, 579–590 (2002).
68. Sobol, I. M. Sensitivity analysis for non-linear mathematical models. *Math. Modell. Comput. Exp.* **1**, 407–414 (1993).
69. Saltelli, A., Tarantola, S., Campolongo, F. & Ratto, M. *Sensitivity Analysis in Practice: A Guide to Assessing Scientific Models* Vol. 1 (Wiley Online Library, 2004).
70. Zhang, T. et al. A global perspective on renewable energy resources: NASA's prediction of worldwide energy resources (power) project. In *Proc. ISES World Congress 2007* Vol. 1–Vol. 5 (eds Goswami, D. Y. & Zhao, Y.) 2636–2640 (Springer, 2009).
71. Stackhouse, P. Jr. et al. *Surface Meteorology and Solar Energy (SSE) Release 6.0 Methodology* version 3.2.0 (NASA, 2016).
72. Stackhouse, P. Jr. et al. Supporting energy-related societal applications using NASA's satellite and modeling data. In *Proc. 2006 IEEE International Symposium on Geoscience and Remote Sensing* (ed. Tsang, L.) 425–428 (IEEE, 2006).
73. *World Development Indicators* (World Bank, accessed 9 June 2022); <https://datacatalog.worldbank.org/dataset/world-development-indicators>
74. Haitz, R. H., Craford, M. G. & Weissman, R. H. In *Handbook of optics* Vol. 2 (ed. Bass, M.) 121–129 (Optical Society of America, 1995).
75. García-Gil, A., Abeledo-Lameiro, M. J., Gómez-Couso, H. & Marugán, J. Kinetic modeling of the synergistic thermal and spectral actions on the inactivation of *Cryptosporidium parvum* in water by sunlight. *Water Res.* **185**, 116226 (2020).

Acknowledgements

This study was funded by the National Science Foundation Nanosystems Engineering Research Center for Nanotechnology-Enabled Water Treatment (EEC-1449500).

Author contributions

J.-H.K. and P.J.J.A. conceived the idea and supervised the work. I.J. designed the analysis, collected the data, implemented overall analysis, interpreted the data and wrote the manuscript and Supplementary Materials. E.C.R. collected the data and contributed to data interpretation and writing Supplementary Materials. All authors contributed to the reviewing and the editing of the manuscript.

Competing interests

The authors declare no competing interests.

Additional information

Supplementary information The online version contains supplementary material available at <https://doi.org/10.1038/s41893-022-00915-7>.

Correspondence and requests for materials should be addressed to Jae-Hong Kim.

Peer review information *Nature Sustainability* thanks Kevin McGuigan and the other, anonymous, reviewer(s) for their contribution to the peer review of this work.

Reprints and permissions information is available at www.nature.com/reprints.

Publisher's note Springer Nature remains neutral with regard to jurisdictional claims in published maps and institutional affiliations.

© The Author(s), under exclusive licence to Springer Nature Limited 2022

Reporting Summary

Nature Research wishes to improve the reproducibility of the work that we publish. This form provides structure for consistency and transparency in reporting. For further information on Nature Research policies, see our [Editorial Policies](#) and the [Editorial Policy Checklist](#).

Statistics

For all statistical analyses, confirm that the following items are present in the figure legend, table legend, main text, or Methods section.

n/a Confirmed

- | | | |
|-------------------------------------|-------------------------------------|--|
| <input type="checkbox"/> | <input checked="" type="checkbox"/> | The exact sample size (n) for each experimental group/condition, given as a discrete number and unit of measurement |
| <input checked="" type="checkbox"/> | <input type="checkbox"/> | A statement on whether measurements were taken from distinct samples or whether the same sample was measured repeatedly |
| <input type="checkbox"/> | <input checked="" type="checkbox"/> | The statistical test(s) used AND whether they are one- or two-sided
<i>Only common tests should be described solely by name; describe more complex techniques in the Methods section.</i> |
| <input checked="" type="checkbox"/> | <input type="checkbox"/> | A description of all covariates tested |
| <input checked="" type="checkbox"/> | <input type="checkbox"/> | A description of any assumptions or corrections, such as tests of normality and adjustment for multiple comparisons |
| <input type="checkbox"/> | <input checked="" type="checkbox"/> | A full description of the statistical parameters including central tendency (e.g. means) or other basic estimates (e.g. regression coefficient) AND variation (e.g. standard deviation) or associated estimates of uncertainty (e.g. confidence intervals) |
| <input checked="" type="checkbox"/> | <input type="checkbox"/> | For null hypothesis testing, the test statistic (e.g. F , t , r) with confidence intervals, effect sizes, degrees of freedom and P value noted
<i>Give P values as exact values whenever suitable.</i> |
| <input checked="" type="checkbox"/> | <input type="checkbox"/> | For Bayesian analysis, information on the choice of priors and Markov chain Monte Carlo settings |
| <input checked="" type="checkbox"/> | <input type="checkbox"/> | For hierarchical and complex designs, identification of the appropriate level for tests and full reporting of outcomes |
| <input checked="" type="checkbox"/> | <input type="checkbox"/> | Estimates of effect sizes (e.g. Cohen's d , Pearson's r), indicating how they were calculated |

Our web collection on [statistics for biologists](#) contains articles on many of the points above.

Software and code

Policy information about [availability of computer code](#)

Data collection

Data analysis

For manuscripts utilizing custom algorithms or software that are central to the research but not yet described in published literature, software must be made available to editors and reviewers. We strongly encourage code deposition in a community repository (e.g. GitHub). See the Nature Research [guidelines for submitting code & software](#) for further information.

Data

Policy information about [availability of data](#)

All manuscripts must include a [data availability statement](#). This statement should provide the following information, where applicable:

- Accession codes, unique identifiers, or web links for publicly available datasets
- A list of figures that have associated raw data
- A description of any restrictions on data availability

All datasets used in this study are publicly available from the cited references in a data availability statement, and codes that support the findings of this study are available from the corresponding author upon reasonable request.

Field-specific reporting

Please select the one below that is the best fit for your research. If you are not sure, read the appropriate sections before making your selection.

Life sciences Behavioural & social sciences Ecological, evolutionary & environmental sciences

For a reference copy of the document with all sections, see [nature.com/documents/nr-reporting-summary-flat.pdf](https://www.nature.com/documents/nr-reporting-summary-flat.pdf)

Ecological, evolutionary & environmental sciences study design

All studies must disclose on these points even when the disclosure is negative.

Study description	We calculate disinfection performance of five different solar-based point-of-use technologies based on each predicted model for each technology. We used some climatic data (e.g., surface solar radiation, temperature), while the other values for all other variables in the model were set based on the references. In addition, we did sensitivity analyses including Morris OAT screening analysis and Sobol's variance-based sensitivity analysis to quantitatively evaluate which parameter of the model for each technology has the greatest influence on the overall disinfection performance and its uncertainty. All details about statistical analyses used in this study and data collection are thoroughly described in the article and Supplementary Materials.
Research sample	All dataset used in this study are publicly available from the cited references in a data availability statement
Sampling strategy	No sample size was chosen, and all data from each dataset (described in the article and Supplementary Materials) were used for the analysis.
Data collection	The data were collected through downloading from the websites.
Timing and spatial scale	Timing and spatial scale of different datasets are various, and all details are summarized in the article and Supplementary Materials.
Data exclusions	No data were excluded from the analysis.
Reproducibility	The analyses were mostly conducted by the R software, while some of the statistical analyses in Supplementary Materials were conducted by GraphPad Prism X9 software. Our study is fully reproducible with the correct codes, and the codes are available from the corresponding author upon reasonable request.
Randomization	Randomization is not relevant to this study, because we did not categorize data into sub-groups and all relevant data were used.
Blinding	Blinding to reduce detection and performance bias is not relevant to this study.
Did the study involve field work?	<input type="checkbox"/> Yes <input checked="" type="checkbox"/> No

Reporting for specific materials, systems and methods

We require information from authors about some types of materials, experimental systems and methods used in many studies. Here, indicate whether each material, system or method listed is relevant to your study. If you are not sure if a list item applies to your research, read the appropriate section before selecting a response.

Materials & experimental systems

n/a	Involvement in the study
<input checked="" type="checkbox"/>	<input type="checkbox"/> Antibodies
<input checked="" type="checkbox"/>	<input type="checkbox"/> Eukaryotic cell lines
<input checked="" type="checkbox"/>	<input type="checkbox"/> Palaeontology and archaeology
<input checked="" type="checkbox"/>	<input type="checkbox"/> Animals and other organisms
<input checked="" type="checkbox"/>	<input type="checkbox"/> Human research participants
<input checked="" type="checkbox"/>	<input type="checkbox"/> Clinical data
<input checked="" type="checkbox"/>	<input type="checkbox"/> Dual use research of concern

Methods

n/a	Involvement in the study
<input checked="" type="checkbox"/>	<input type="checkbox"/> ChIP-seq
<input checked="" type="checkbox"/>	<input type="checkbox"/> Flow cytometry
<input checked="" type="checkbox"/>	<input type="checkbox"/> MRI-based neuroimaging